Supplementary material to referees' response to A model based constraint of CO2 fertilisation, Holden et al

Figure 1

The upper panels plot the CMIP5 forcing data of the change in LUC fraction from 1900 to 2000, separated into crop and pasture.

The lower panel plots the combined CMIP5 data (summed change in crop and pasture fraction) integrated onto the GENIE grid.

Figure 2

The upper panels illustrate the preindustrial (850 AD) vegetation and soil carbon densities simulated by GENIE. The data is the average of a 20-member ensemble, described in Joos et al (2012), a filtered subset of "Ensemble 1" (see manuscript).

The bottom plot is the LUC change (as Fig 1). The comparison highlights the regions where we may expect dominant LUC emissions (both high potential carbon density and large LUC change).

Figure 3

The upper panels plot the change in vegetation and soil carbon densities from 1900 to 2000 due to LUC. These data (Eby et al 2012) are derived from the 20-member ensemble, from simulations with only LUC forcing (CO_2 is relaxed to 280ppm). These data isolate the LUC forced change from the climate and CO_2 fertilisation forced changes. Note that they do not isolate the directly forced LUC change from LUC-driven climate feedbacks. Regions of increased soil density are likely the result of LUC-climate feedbacks, being regions where local cooling leads to decreased soil respiration that outweighs the direct LUC effect (decreased leaf litter input to the soil). This is discussed further with respect to Figs 6 and 8.

The largest LUC-forced changes are due to tropical deforestation and central USA deforestation. The changes are dominantly in vegetation carbon, although though there are large soil carbon changes in central USA and in the Himalayas. The Himalayan soil changes may be unreasonably high. These arise due to high potential soil densities at high altitudes due to lapse rate cooling. We note that soil weathering is not modelled. The Central USA vegetation changes may also be somewhat high, arising from a high potential vegetation carbon density (Fig 2). This is likely due to excessive moisture transport into the continental interior by the diffusive EMBM atmosphere.

The lower panel again plots the LUC forcing, shown for ease of comparison.

Figure 4

A comparison between observational data (Olsen et al 1985, upper panels), preindustrial (850 AD) ensemble-averaged (middle panels) and modern LUC-forced ensemble-averaged (lower panels). Left: vegetation carbon density, right: soil carbon density.

The distributions are generally quite reasonable and vegetation density has been brought closer to observations by the inclusion of LUC (thinning of tropical forest, central USA and Europe). Note that boreal forests are not well represented in the model, although this is unlikely to be a major issue for our purposes here as these regions are largely unaffected by LUC.

Figure 5

Average LUC-forced land-atmosphere carbon fluxes (1900-2000). Left panel plots GENIE (20-member ensemble-average, LUC forcing only). Right panel plots the observationally-driven data of Raddatz (2010). These data are scaled to match the bookkeeping estimates of Houghton (2008, tabulated in lower panel), locally weighted by population (capped at 20 persons per km^2).

The agreement is generally reasonable, especially given that spatial differences are expected; highest emissions in Raddatz are associated with high population density, highest emissions in GENIE are associated with regions of previously dense vegetation.

Although the map comparison suggests that GENIE overestimates tropical African emissions, the comparison with Houghton (9% of global emissions) is favourable. The emissions from central USA are overstated in GENIE (see discussion for Figure 3).

Figure 6

The upper panel compares the 20-member LUC-forced GENIE LUC emissions time series with the bookkeeping time series of Houghton (2008) and the estimate of LPJmL (9-year running mean of a new analysis which we have performed to assist this validation). GENIE appears to underestimate the LUC flux, especially in recent decades.

The lower panel is a similar comparison (solid lines) that includes all the AR5 EMICs which model LUC, reproduced from Eby et al (2012). Understated recent emissions appear to be a general feature of the EMICs, although UVic (red) matches Houghton more closely. Note that the error estimates for Houghton (vertical grey bars) suggest possible consistency, although the majority of the EMICs are at the limits of the Houghton uncertainty range. A detailed investigation of the sources of these differences may be beyond the scope of this paper, although we will make efforts to address them. They likely include different potential vegetation distributions, different treatments of the effect of LUC on soil carbon and different rates at which vegetation is restored to natural levels in previously LUC affected regions that are now recovering.

We note that the EMIC data is not directly analogous to either the Houghton or LPJmL analyses because the EMICs include LUC-driven climate feedbacks. We are presently investigating the potential role of these feedbacks in the robustness of this validation and will refine our discussion (and analysis), if necessary.

Figure 7

The LUC forcing profile leads to the temporal profile in Fig 6. Four decadal changes of fractional LUC are plotted. Land use fraction increases greatly from 1950 to 1960 (associated with the sharp peak in Fig 6) and generally increases from 1979 to 1989 (associated with a secondary peak in Fig 6). There are large regions post-1960 that have been monotonically reverting to their natural state, the likely cause of the simulated LUC flux reduction in recent times. Note that ENTSmL assumes instantaneous reforestation when previously LUC-affected land is no longer cultivated (of which 50% carbon comes from soil and 50% from atmosphere). This is likely to be part of the explanation for the reduced GENIE flux in this period.

Figure 8

Parameter KC is the fractional reduction in leaf litter input to soils under LUC. This is critical for LUC emissions as demonstrated in this plot of total LUC emissions (1850-2000) against KC. This suggests that rather than applying a prior, we should instead calibrate KC based on historical LUC emissions. Houghton emissions of 149GTC suggest that the KC prior should be centred on ~0.45 (not 0.2 as was used in the submitted manuscript). We note that the highest value of KC in this 20-member ensemble is 0.55. This 20-member ensemble was filtered from a 100-member ensemble with KC in the range 0.0 to 1.0. The requirement for plausible 2000 CO_2 has imposed a strong constraint on the upper limit of KC. From a linear fit to these points, a Gaussian "prior" for KC appears reasonable, centred on 0.45 with a standard deviation of 0.11. The 90% confidence interval spans the range 0.23 to 0.67. Outside of this range, LUC emissions are difficult to reconcile with plausible 2000 CO_2.

This revised prior was performed by consideration of the Houghton data. An alternative is to derive the prior based on the LPJmL simulation, producing a prior centred upon 0.54. This alternative will be used to provide sensitivity analysis for the calibration in the revised manuscript.

What does uncertainty in KC represent? By design, this parameter was intended to parameterise the effects of crops on soil carbon. Soil carbon is reduced under cropped land as harvesting reduces the carbon returned to the soil and tillage increases soil oxidation rates. However, if KC is to be regarded as a tuning parameter for the LUC model, then appropriate values will also subsume structural deficiencies of ENTSmL. Most notably, the ENTS soil model has a single layer that reacts instantaneously throughout its depth to surface temperature changes. LUC results in a local radiative cooling due to increased albedo, and it is likely that an excessive decrease in soil respiration (and increase in soil carbon density) would result. As such, the relatively high values of KC

needed to explain LUC emissions is likely due, at least in part, to this sensitive soil carbon response to LUC (both crop and pasture). i.e. a reduction in leaf-litter input (an increase in KC) may be required to simulate realistic soil carbon densities under LUC. Note that the calibration of KC is also required to subsume other structural deficiencies, such as the excessive potential vegetation in central USA, or the excessive potential soil carbon at high-altitude.

Figure 9

The pdf of CO_2 fertilisation, based on various sensitivity analyses.

The left panel compares sensitivities to the prior assumption:

Purple: approximately the calibration in the submitted paper (KC prior centred on 0.2). It differs slightly as we now constrain for a CO_2 increase of 84ppm (c.f. 90ppm in the manuscript), better reflecting the observational change from 1850 to 2000.

Blue: new base case, as purple but with the KC prior centred on 0.45.

Light blue: as new base case but with the KC prior centred on 0.54.

Green: as new base case but with a uniform KC prior.

The right panel compares sensitivities to the structural error assumptions:

Turqoise: as new base case but with a structural bias term in the calibration to allow for the underestimate of LUC emissions compared to Houghton. Note that even with the KC prior, a small low bias with respect to Houghton remains, although the calibration is relatively insensitive to this (compare turquoise and blue curves).

Orange: as turquoise, but now the prior is centred on 0.2 and the bias correction is increased (as with this assumption there is a greater discrepancy with Houghton, see Fig 8). Note that this calibration is very similar to turquoise, so either adjusting the KC prior or correcting through the bias term appear to have a similar effect on the calibration.

Red: as new base case but neglecting structural error.

It is apparent that the KC=0.45 pdf is quite insensitive to these various assumptions, although it is somewhat different from the (KC=0.2) pdf in the submitted manuscript. We now have greater LUC emissions so that higher CO2 fertilisation is required to reproduce the observed CO2. We note that negligible CO_2 fertilisation now becomes even more difficult to reconcile with the analysis.

Figure 10

Temporal evolution of atmospheric CO_2. Red is observed. Green is the ensemble-averaged evolution, now an average over the 670-member ensemble (all forcings). Blue is probability weighted by the calibration. In the calibrated curve, CO_2 is well matched as expected, although underestimated by 5-10ppm between 1850 and 1950. The sharp drop in CO_2 at 1815 is associated with the Tambora volcanic eruption and reflects the unreasonably fast response time of ENTS soil carbon to surface cooling (see text describing Fig. 8). However, the comparably rapid recovery suggests that this is unlikely to explain the low CO_2 estimates that persist through to 1950. A more likely explanation is the underestimate of early LUC emissions (Fig 6). The LUC emissions spike from 1950-1960 reconciles both the temporally integrated emissions and the CO_2 concentration.

Figure 11

On the left are the calibrated outputs in the submitted manuscript. On the right are the revised calibrations (DeltaCO_2 84ppm, KC centred on 0.45). The most noticeable difference is that net LUC emissions (1990-2000) are now less likely (right middle panel). Increasing KC (prior centered on 0.45, rather than 0.2) increases LUC emissions, but these additional emissions are dominantly at early times. The calibration increases CO_2 fertilisation to compensate. This approximately balances the time-integrated LUC emissions and CO_2 fertilisation uptake in order to preserve atmospheric CO_2, but the additional uptake is dominantly at later times when CO_2 is highest. This timing difference likely explains the shift in the pdf for 1990-2000.

These figures now also include the results from two LPJmL simulations, one with CO_2 fertilisation (dark green vertical bars) and the other without CO_2 fertilisation (light green vertical bars). It is apparent that reasonable land-atm fluxes can only be generated under the assumption of CO2 fertilisation in (this configuration of) LPJmL.

References

Eby et al, 2012, Historical and idealised climate model experiments: an EMIC intercomparison, Clim. Past Discuss., 8, 4121-4181

Houghton, 2008, Carbon flux to the atmosphere from land-use changes: 1850-2005. In TRENDS: A Compendium of Data on Global Change, Carbon Dioxide Information Analysis Centre, Oak Ridge National Laboratory, Tennessee

Joos et al, 2012, Carbon dioxide and climate impulse response functions for the computation of greenhouse gas metric: a multi-model analysis, Atmos. Chem. Phys. Discuss, 12, 19799-19869

Olsen et al, 1985, Major world ecosystem complexes ranked by carbon in live vegetation, NDP-017, Carbon Dioxide Information Analysis Centre, Oak Ridge National Laboratory, Tennessee

Raddatz, 2010, Historical landcover change and wood harvest CO_2 emissions, MPI for Meteorology, Hamburg, Germany.
www.mpimet.mpg.de/en/wissenschaft/land-im-erdsystem/wechselwirkung-klima-biogeosphaere/landcover-change-emission-data.html

Williamson et al, 2006, An efficient numerical terrestrial scheme (ENTS) for Earth system modelling, Ecological modelling, 198, 362-374

Crop change (1900 to 2000)

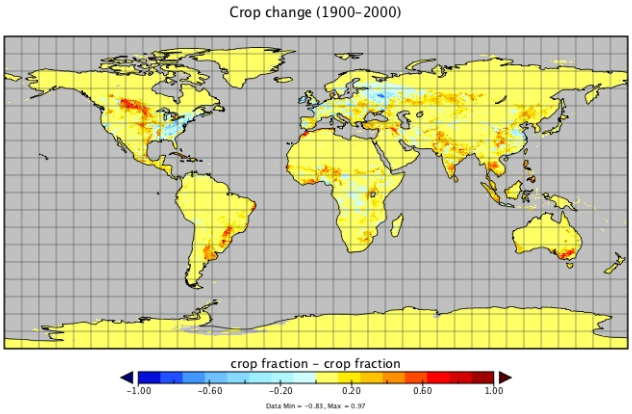

Pasture change (1900 to 2000)

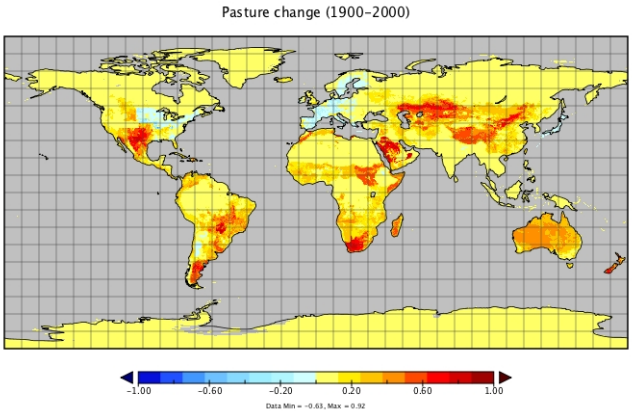

CMIP5

GENIE

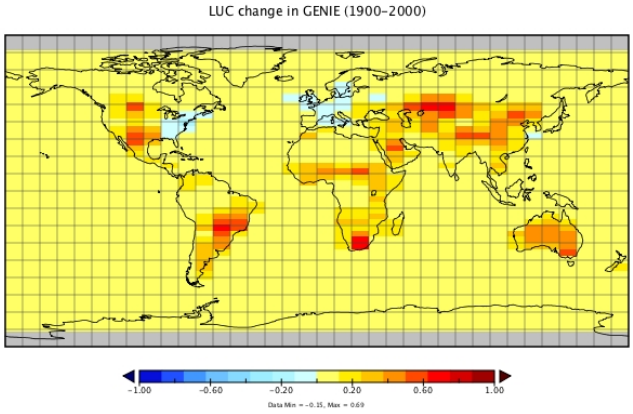

1

LUC change (1900 to 2000) (fractional coverage)

PI (850AD) vegetation carbon density kgCm-2

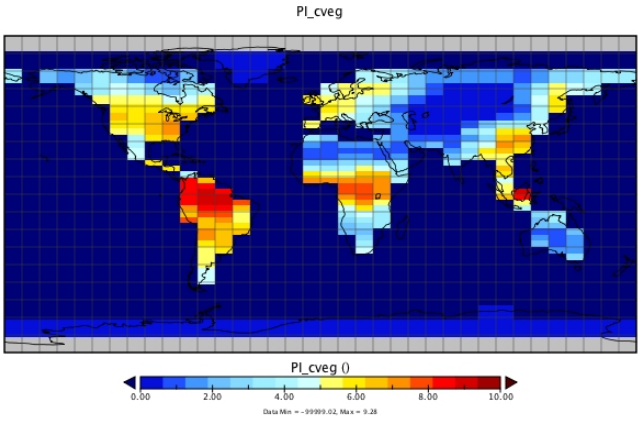

PI (850AD) soil carbon density kgCm-2

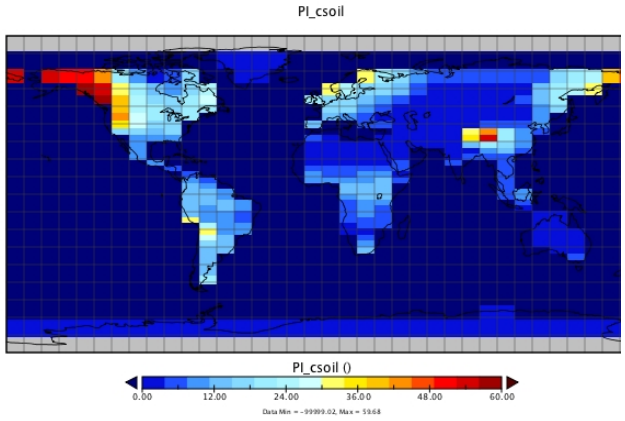

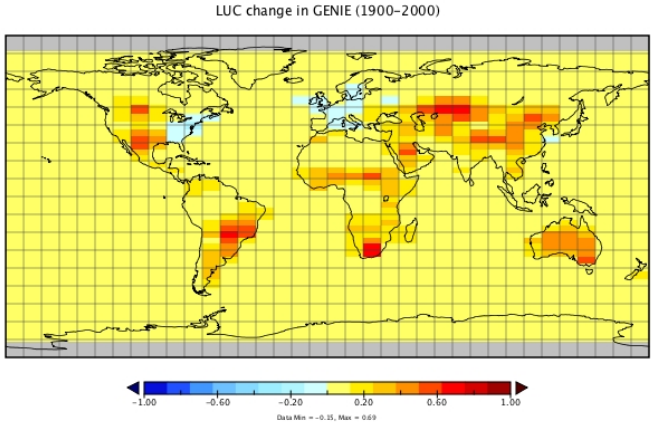

LUC change (1900 to 2000) (fractional coverage)

Change in Cveg density (1900 to 2000)

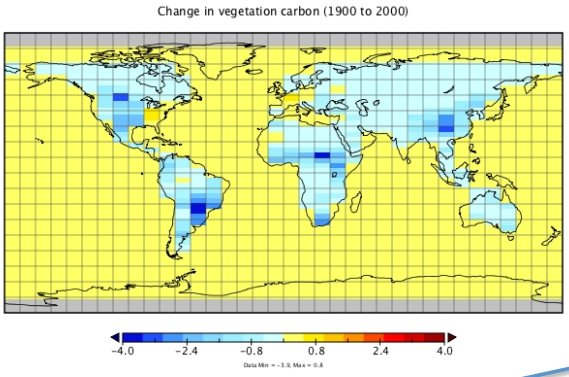

Change in Csoil density (1900 to 2000)

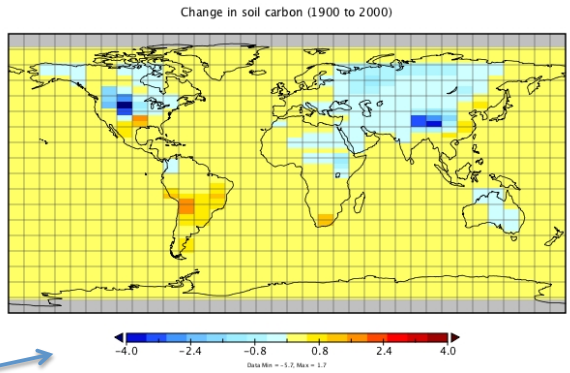

LUC forcing only

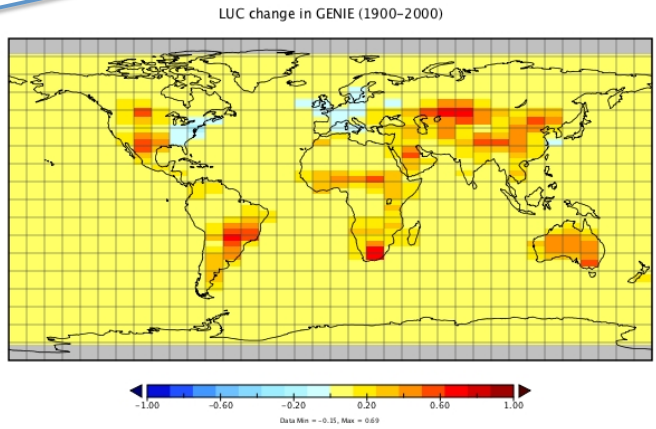

LUC change (1900 to 2000) (fractional coverage)

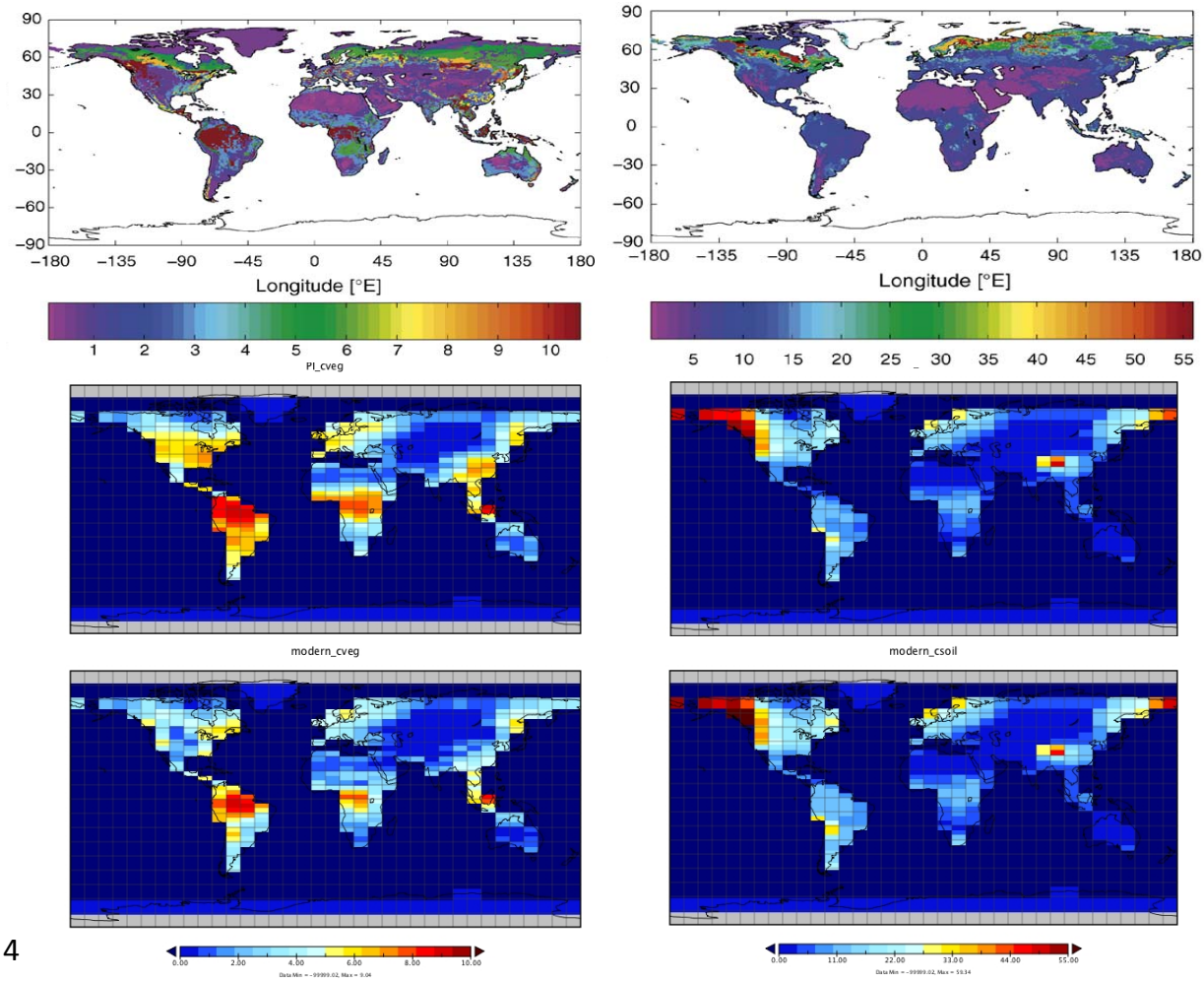
90
60
30
0
−30
−60
−90
−180 −135 −90 −45 0 45 90 135 180
Longitude [°E]
1 2 3 4 5 6 7 8 9 10
PI_cveg
5 10 15 20 25 30 35 40 45 50 55
modern_cveg
modern_csoil
0.00 2.00 4.00 6.00 8.00 10.00
0.00 11.00 22.00 33.00 44.00 55.00

LUC land-atmosphere flux (1900-2000 average, $gCm^{-2}s^{-1}$)

GENIE

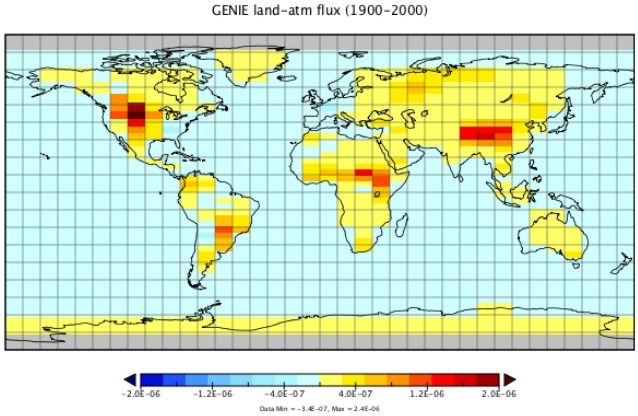

Observationally-driven (Raddatz 2010)

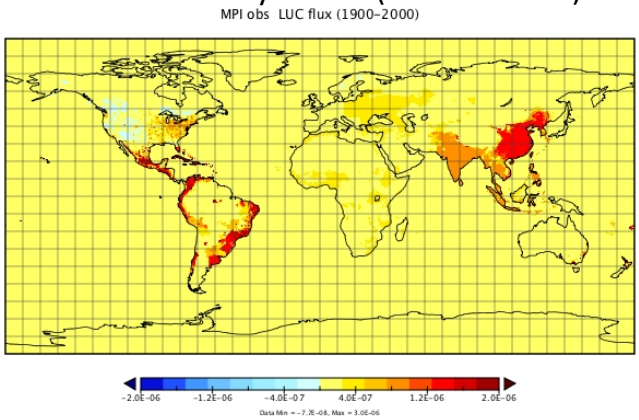

Observationally-driven book-keeping model (Houghton, 2008)

Total LUC emissions by region (1900-2000, GTC)

Global	USA	Canada	S&C America	Europe	N Africa	Trop Africa	USSR	China	S&SE Asia	Pac
116.9	2.5	3.6	36.7	2.3	2.7	10.9	8.0	20.5	26.3	

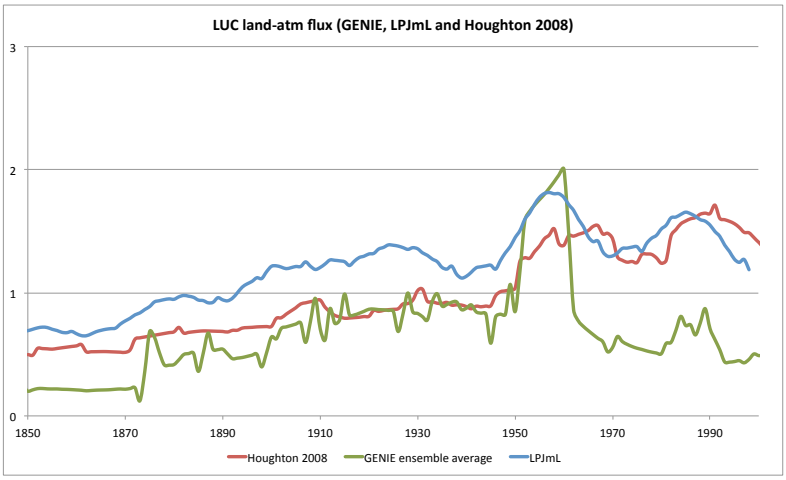
LUC land-atm flux (GENIE, LPJmL and Houghton 2008)
3
2
1
0
1850
1870
1890
1910
1930
1950
1970
1990
Houghton 2008
GENIE ensemble average
LPJmL

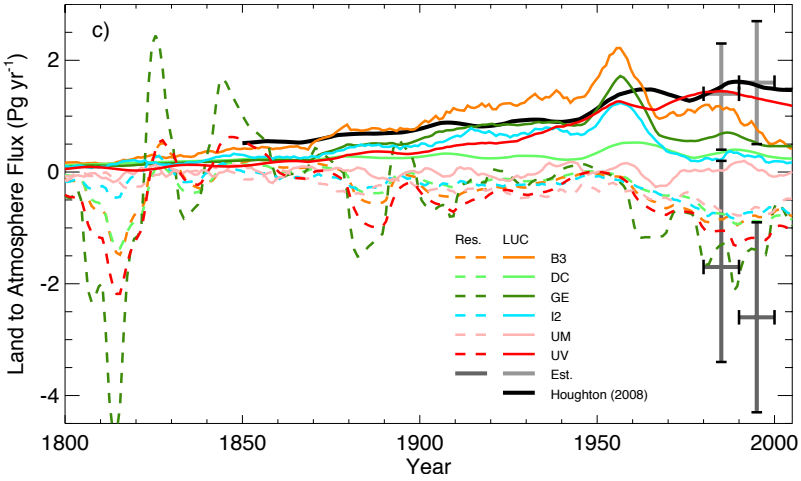
c)
Land to Atmosphere Flux (Pg yr-1)
2
0
-2
-4
1800
1850
1900
1950
2000
Year
Res.
LUC
B3
DC
GE
I2
UM
UV
Est.
Houghton (2008)

LUC_fraction_change (1950 to 1960)

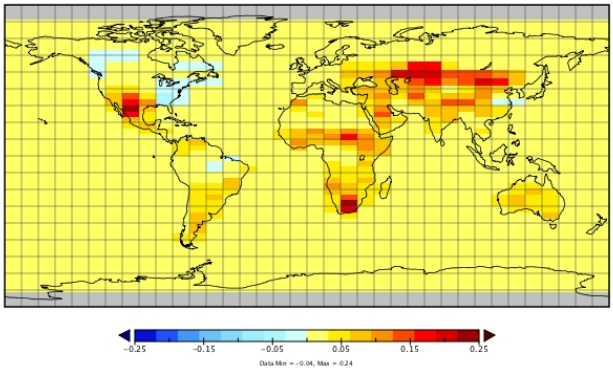

LUC_fraction_change (1960 to 1970)

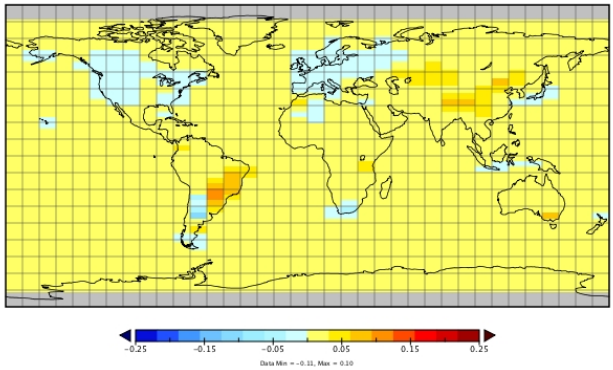

LUC_fraction_change (1979 to 1989)

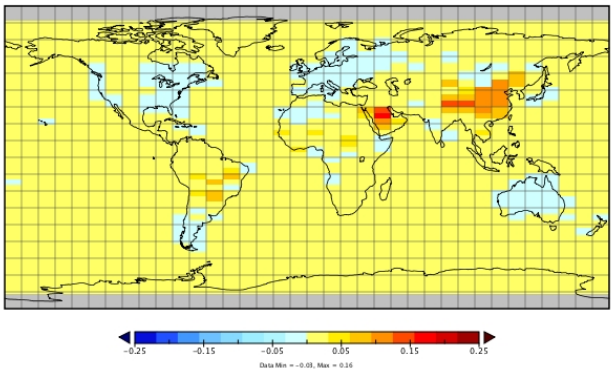

LUC_fraction_change (1989 to 1999)

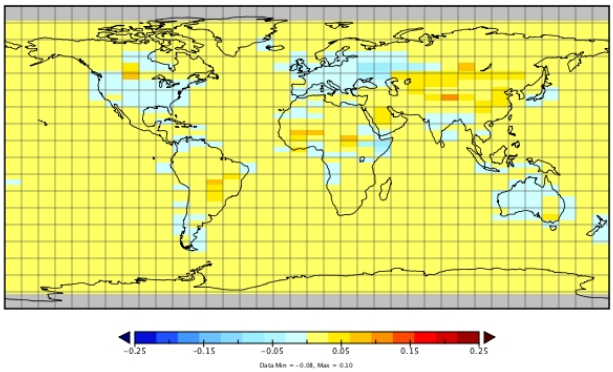

KC is the fractional reduction in leaf litter under LUC, a very important driver of uncertainty in LUC emissions. This suggests a possible calibration target for KC. Houghton (2008) LUC emissions of 149 GTC (1850 to 2000) suggests KC ~ 0.4

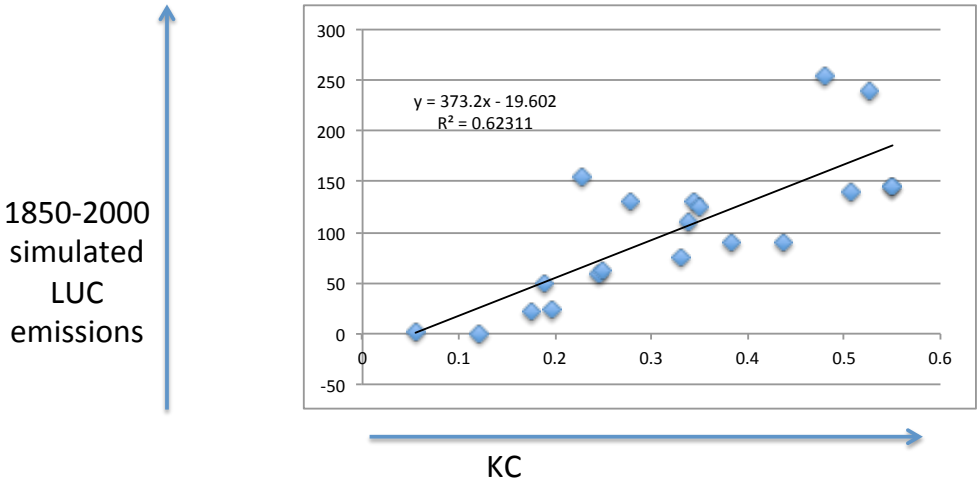

CO2 fertilisation posterior

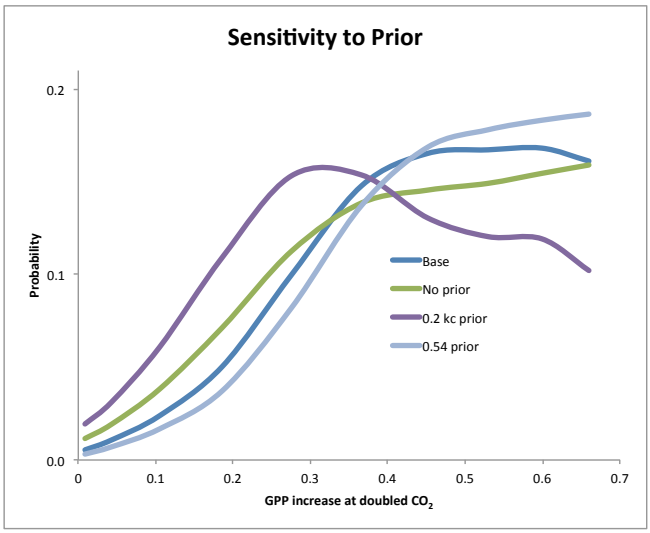

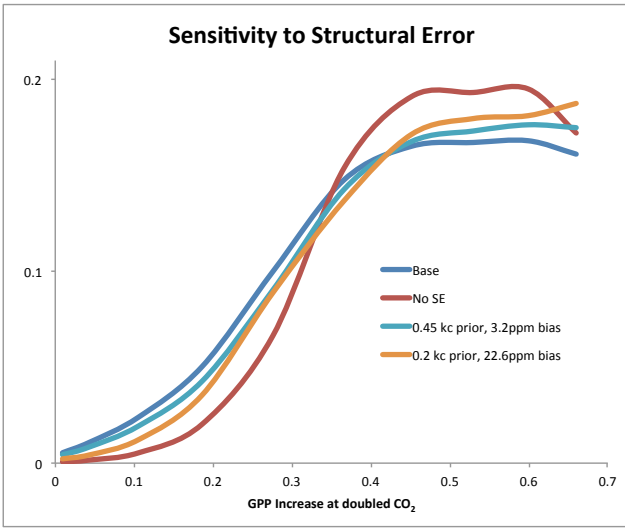

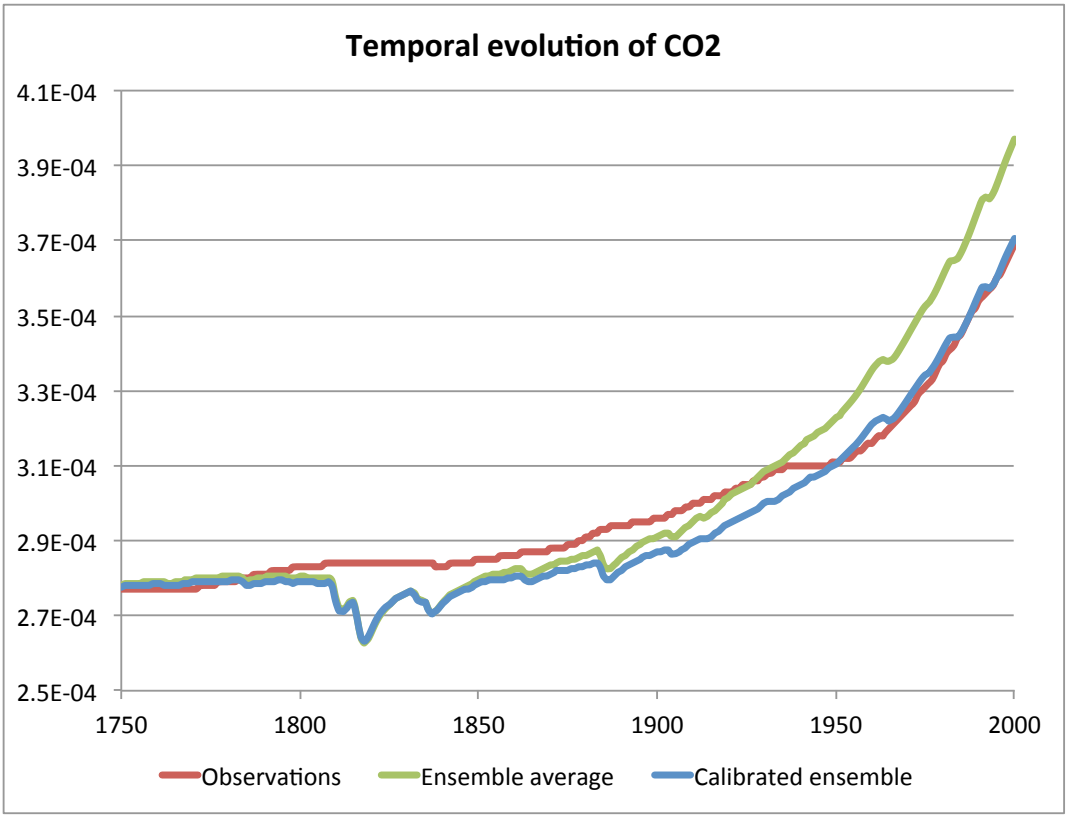
Temporal evolution of CO2
4.1E-04
3.9E-04
3.7E-04
3.5E-04
3.3E-04
3.1E-04
2.9E-04
2.7E-04
2.5E-04
1750
1800
1850
1900
1950
2000
Observations
Ensemble average
Calibrated ensemble

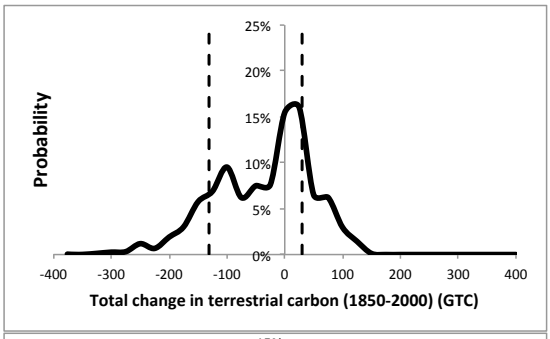
Probability
25%
20%
15%
10%
5%
0%
-400 -300 -200 -100 0 100 200 300 400
Total change in terrestrial carbon (1850-2000) (GTC)

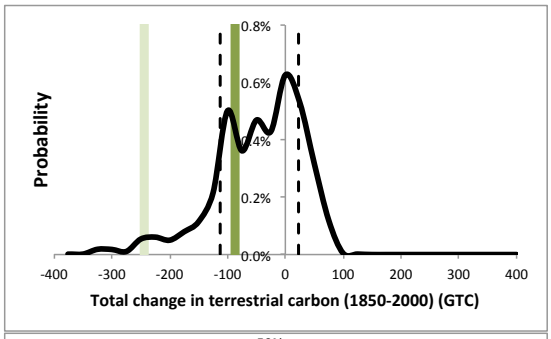
Probability
0.8%
0.6%
0.4%
0.2%
0.0%
-400 -300 -200 -100 0 100 200 300 400
Total change in terrestrial carbon (1850-2000) (GTC)

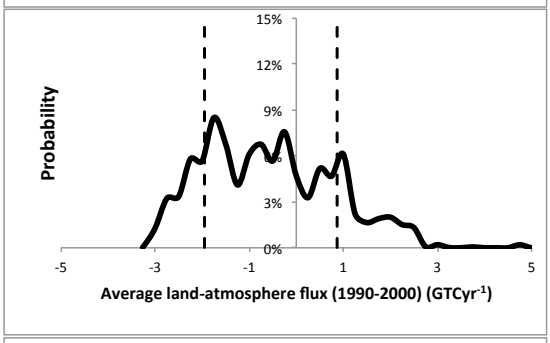
Probability
15%
12%
9%
3%
0%
-5 -3 -1 1 3 5
Average land-atmosphere flux (1990-2000) (GTCyr-1)

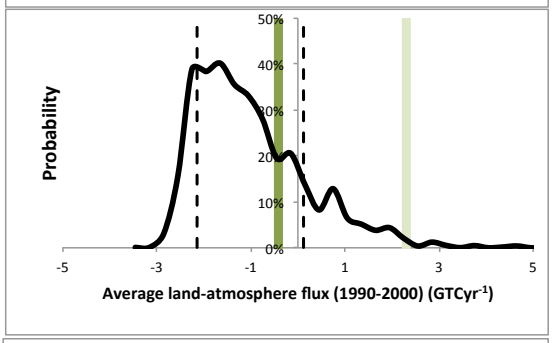
Probability
50%
40%
10%
0%
-5 -3 -1 1 3 5
Average land-atmosphere flux (1990-2000) (GTCyr-1)

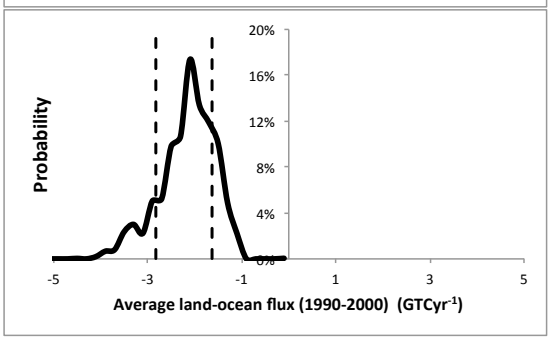
Probability
20%
16%
12%
8%
4%
-5 -3 -1 1 3 5
Average land-ocean flux (1990-2000) (GTCyr-1)

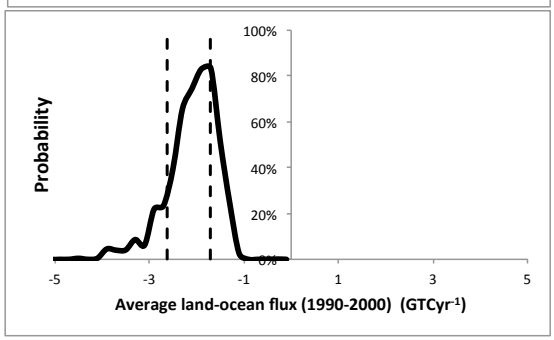
Probability
100%
80%
60%
40%
20%
0%
-5 -3 -1 1 3 5
Average land-ocean flux (1990-2000) (GTCyr-1)